Journal of Materials Chemistry C

Accepted Manuscript

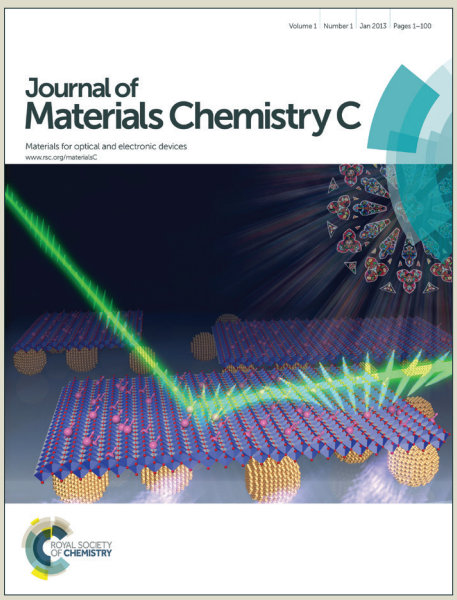

ROYAL SOCIETY OF CHEMISTRY

www.rsc.org/materialsC

Journal Name

ARTICLE

Ratiometric multiplexed barcodes based on luminescent metal-organic framework films

Received 00th January 20xx,
Accepted 00th January 20xx

DOI: 10.1039/x0xx00000x

www.rsc.org/

You Zhou,[a] Bing Yan,*[a]

Herein, a new MOF barcoded system is developed based on lanthanides photofunctionalized MOF films that contain multiple emission bands. The encoding strategy is based on tuning the emission intensity of lanthanides MOFs in multiple bands via the encapsulation of a screen layer containing different amounts of organic dyes. By controlling the filtered dyes loading, we can predict and tune the emissions of Ln^{3+}@MIL-100 (In) films in multiple bands and therefore give rise to distinct ratiometric optical codes. This work highlights the opportunity of lanthanides luminescence MOFs for generating barcodes in a reproducible and robust way. In addition, spectral encoding relied on lanthanides luminescence offers a range of advantages over organic fluorophores and quantum dots, such as low spectra and background interference, and self-referencing.

Introduction

Luminescent barcoded materials are very attractive in industrial functions such as anti-counterfeiting, multiplexed bioanalytical assays, and forensic labelling. To date, spectral barcoding has primarily been done with both organic dyes[1-4] and inorganic quantum dots[5-10] that embedded into polymers or silica microbeads. However, organic fluorophores have broad emission bands which results spectra overlap of different organic dyes, and therefore a limited number of wavelengths are available for barcoding. The wavelengths of quantum dots are relatively narrow, and can be modulated by bandgap engineering, [6,11,12] but quantum dots are generally made of toxic materials (e.g., CdS, CdSe, CdTe). Lanthanides luminescent materials have unique advantages in comparison with the barcodes of organic dyes and inorganic quantum dots. Specifically, the emission bands are narrow, nonoverlapping and well-resolved. Besides, the emission wavelengths depend only on the nature of lanthanides cations.[13] It enables the lanthanides luminescence barcodes to use in various materials and solvent where their emission wavelengths are not influenced. Optical barcodes based on lanthanides-doped inorganic nanocrystals have been frequently addressed. [14-17]

As a new class of lanthanides luminescent materials, lanthanides luminescent metal-organic frameworks (MOFs) featuring permanent, well-defined porosity and intensive fluorescence have gathered considerable attention in the past few years.[18-22] Most efforts were directed toward the synthesis of lanthanides luminescence MOFs and their applications in chemical sensors,[23-27] light-emitting devices.[28-32] Recently, a new barcoding use was demonstrated in lanthanides luminescence MOFs.[33,34] The first lanthanides luminescence MOF barcode was developed by White and co-workers, which is based on polymetallic lanthanide MOFs that emit several independent NIR fluorescent signals arising from different lanthanide cations.[33] By controlling the reactant stoichiometry, the authors can tune the lanthanides composition of the polymetallic MOF and therefore control the resulting emission intensity of the individual signals of the lanthanide cations. By employing the same encoding strategy, another lanthanide luminescence MOF barcoded system was achieved recently.[34] In this contribution, we have developed a new barcoded system based on lanthanides photo-functionalized MOF films that contain multiple emission bands. Our encoding strategy relies on tuning

Scheme 1. Schematic illustration of the encoding strategy based on tuning the multiple emission bands of lanthanides luminescent MOFs. Blue and red emissions can be tuned by controlling filtered dyes loading, while the green emission is not adsorbed and serves as an internal reference to generate ratiometric optical codes.

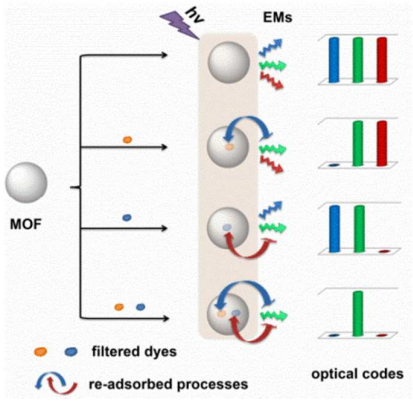

[a] Shanghai Key Lab of Chemical Assessment and Sustainability, Department of Chemistry, Tongji University, Siping Road 1239, Shanghai 200092, China. E-mail: byan@tongji.edu.cn;

† Electronic Supplementary Information (ESI) available. See DOI: 10.1039/x0xx00000x

the emission intensities of lanthanides in multiple bands through luminescence re-absorbed processes (Scheme 1), which is significantly different from that of the two previously reported MOF barcoded systems. Varying the filtered dyes loading generates distinct ratiometric optical signatures or codes. Ratiometric luminescence measurements are independent of excitation power fluctuations, the optoelectronic drift of the detectors, and material's inhomogeneities. Therefore, our new strategy allows the construction of MOF luminescence barcodes in a reproducible and robust way.

Experimental Section

Materials and methods

All chemicals were purchased from commercial sources and used without purification. $InCl_3 \cdot 4H_2O$ was purchased from Aldrich. Trimesic acid and methylene blue (MB) were purchased from Adamas. Fluorescein isothiocyanate (FL) were purchased from Acros. Lanthanide chlorides were obtained from the corresponding oxides in HCl (37.5%).

Powder X-ray diffraction patterns (PXRD) were recorded with a Bruker D8 diffractometer using CuKα radiation with 40 mA and 40 kV. X-ray photoelectron spectroscopy (XPS) experiments were carried out on a RBD upgraded PHI-5000C ESCA system (Perkin Elmer) with MgKa radiation ($h\nu$ = 1253.6 eV). Inductively coupled plasma-mass spectrometry (ICP-MS) data were collected on an X-7 series inductively coupled plasma-mass spectrometer (Thermo Elemental, Cheshire, UK), the samples were prepared by digesting the dry samples of Ln^{3+}@MIL-100 (In) films into concentrated HNO_3, followed by the dilution to 0.5% HNO_3 solution. The morphologies of samples were characterized by Field emission scanning electron microscopy (FESEM, Hitachi S4800). UV–vis absorption spectra were obtained a Shimadzu 3000 spectrophotometer. The photoluminescence spectra and luminescent decay times were examined by an Edinburgh FLS920 phosphorimeter. The absolute external luminescent quantum efficiency was determined employing an integrating sphere (150 mm diameter, BaSO4 coating) from an Edinburgh FLS920 phosphorimeter. The excitation wavelengths of the measurements of the decay times and emission quantum yields were provided in Table S2. The estimated errors for decay times and quantum yields are within 5%.

Synthesis of MIL-100 (In) film

MIL-100 (In) Film was prepared from an in situ solvothermal synthesis method reported by Dou and co-workers.[35] ITO glass (1 × 1 cm^2) was cleaned by ultrasonic bath in DMF and ethanol for three times. Then the cleaned ITO glass was placed in a mixed solution in a 20 ml Teflon-lined stainless steel container, which was prepared by dissolving $InCl_3 \cdot 4H_2O$ (0.044 g, 0.2 mmol) and trimesic acid (0.042 g, 0.2 mmol) in H2O (4 mL), ethanol (5 mL), and DMF (5 mL). After the reaction at 120 °C for 24 h, the resulted film was separated from the mixed dispersion and washed with DMF and ethanol, followed by drying at 25 °C under vacuum.

Synthesis of Ln^{3+}@MIL-100 (In) films

Ln^{3+}@MIL-100 (In) films were prepared by immersing MIL-100 (IN) films in 3 mL ethanol solutions of chloride salts of Ln^{3+} at 25 °C for 48 h. The resulted Ln^{3+}@MIL-100 (In) films were washed with DMF and ethanol, followed by drying at 25 °C under vacuum. For the synthesis of Eu^{3+}@MIL-100 (In) and Tb^{3+}@MIL-100 (In) films, the $LnCl_3$ ethanol solutions used are $EuCl_3$ (o.2 $mol \cdot L^{-1}$) and $TbCl_3$ (o.2 $mol \cdot L^{-1}$), respectively. For the synthesis of Eu^{3+}/Tb^{3+}@MIL-100 (In), $LnCl_3$ ethanol solution was mixed from 2.5 mL $EuCl_3$ (o.2 $mol \cdot L^{-1}$) and $TbCl_3$ (o.2 $mol \cdot L^{-1}$).

Loading dyes into Ln^{3+}@MIL-100 (In) films for barcoding

Encoding Tb^{3+}@MIL-100 (In) films: Tb^{3+}@MIL-100 (In) films were soaking in ethanol solutions of fluorescein isothiocyanate with various concentrations for 12 h in the dark, which affords FL labeled Tb^{3+}@MIL-100 (In) films. FL solutions were prepared by adding 0.1, 0.5, 1 mL of 0.01 mg/mL FL ethanol solution in 3 mL ethanol. The resulted dye loaded films were defined as A_1, A_2, A_3 in the sequence of increased dye concentration. For comparison, the isolated Tb^{3+}@MIL-100 (In) film was defined as A_0. The contents of the loaded FL of the MOF films were estimated by the method described in supporting information, and the results were provided in Table S1

Encoding Eu^{3+}@MIL-100 (In) films: Eu^{3+}@MIL-100 (In) films were soaking in ethanol solutions of methylene blue with different concentrations for 12 h in the dark, which affords MB labeled Tb^{3+}@MIL-100 (In) films. MB ethanol solutions were prepared by adding 0.05, 0.5, 2 mL of 0.1 mg/mL MB ethanol solution in 3 mL ethanol. The resulted MB loaded films were defined as B_1, B_2, B_3 in the sequence of increased dye concentration. For comparison, the isolated Eu^{3+}@MIL-100 (In) film was defined as B_0. The contents of the loaded MB of the MOF films were estimated by the method described in supporting information, and the results were provided in Table S1.

Encoding Eu^{3+}/Tb^{3+}@MIL-100 (In) films: For labeling with FL and MB dyes, Eu^{3+}/Tb^{3+}@MIL-100 (In) films were soaking in mixed ethanol solutions of FL and MB with various concentration combinations. The setting of FL concentrations is the same as that used in labeling Tb^{3+}@MIL-100 (In) films. The setting of MB concentrations, in a similar way, is the same as that employed in labeling Eu^{3+}@MIL-100 (In) films. The resulted encoded Eu^{3+}/Tb^{3+}@MIL-100 (In) films were defined as $A_{x(0-3)}B_{y(0-3)}$, which is correlated to the loading dyes and their concentrations. For instance, A_0B_0 means the free labeled Eu^{3+}/Tb^{3+}@MIL-100 (In) film, and A_0B_3 represents Eu^{3+}/Tb^{3+}@MIL-100 (In) film only labeled with maximum amounts of MB. Considering the feeding concentrations of MB and FL enthanol solutions are the same as that used to encoding Tb^{3+}@MIL-100 (In) film and Eu^{3+}@MIL-100 (In) films, respectively, the content of dyes in Eu^{3+}/Tb^{3+}@MIL-100 (In) films can refer to that in Tb^{3+}@MIL-100 (In) film and Eu^{3+}@MIL-100 (In) films.

Results and discussion

As the MOF we chose a robust MIL-type framework, MIL-100 (In). This framework is characterized by the MTN[36] zeolite-type structure (ZSM-39) with two types of cavities (inner diameters are about 20 and 26 Å (Figure 1a).[37] Specifically, we configured MIL-100 (In) as a transparent thin film on an ITO glass. The synthesis of MIL-100 (In) film was accomplished by an in situ solvothermal method reported

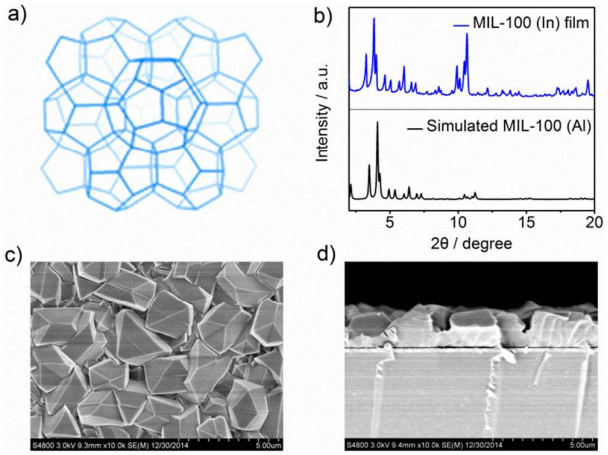

Figure 1. (a) Topological view of MIL-100 (In) with MTN-type zeolitic architecture. (b) Powder X-ray diffraction patterns of simulated MIL-100 (Al) and MIL-100 (In) film. (c) SEM image (top view), and (d) SEM image (cross section) of MIL-100 (In) film. The scale bar in (c) and (d) is 5 um.

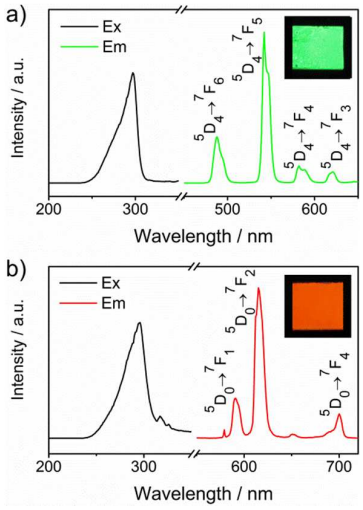

Figure 2. Photoluminescence spectra of Tb^{3+}@MIL-100 (In) (a) and Eu^{3+}@MIL-100 (In) (b) films. The insets in (a) and (b) are the photograph of Tb^{3+}@MIL-100 (In) and Eu^{3+}@MIL-100 (In) films under UV irradiation, respectively.

by Dou and co-workers.[35] The obtained MIL-100 (In) film is transparent and stable for months in air (Figure S3). Powder X-ray diffraction (PXRD) result shows the as-prepared film to be isostructural with MIL-100 (Al) (Figure 1b). The morphology of MIL-100 (In) film is investigated by scanning electron microscopy (SEM). As shown in Figure 1c, MIL-100 (In) film is dense and continuous, and the MOF microcrystals pack tightly. The MOF film maintains integrity upon ultrasonic washing in the water or ethanol for 30 min, indicating the good adhesion between the MOF layer and surface of the ITO glass. According to the previous studies,[37] the indium oxide on the ITO substrate is indispensable for the formation of continuous and robust MOF film, because of that the indium oxide can also serve as indium source during the generation of small MOF crystals and thus improving the homogenous nucleation and growth. The thickness of the MOF film is about 2 um (Figure 1d).

It has been established that extra trimesic acid ligands are existed in the cavities of MIL-100 type framework, and they have strong interaction with the In_3O trimer.[36-39] We reasoned that the extra ligands containing free carboxyl groups can serve as scaffolds to host and sensitize lanthanide cations (Ln^{3+}), thus imparting intense lanthanides luminescence to MIL-100 (In). With this in mind, MIL-100 (In) films were immersed in ethanol solutions of chloride salts of Eu^{3+} and Tb^{3+}, which afford Eu^{3+}@MIL-100 (In) and Tb^{3+}@MIL-100 (In) films. Inductively coupled plasma-mass spectrometry (ICP-MS) analyses of Eu/In and Tb/In of the digested Ln^{3+}@MIL-100 (In) films provided Eu^{3+} and Tb^{3+} loadings of 21.4% and 18.3% for Eu^{3+}@MIL-100 (In) and Tb^{3+}@MIL-100 (In) films, respectively. PXRD patterns of the isolated MIL-100 (In) and Ln^{3+}@MIL-100 (In) films are considerably identical, indicating that the crystal structure of framework 1 is retained in Ln^{3+} functionalized samples (Figure S4). The morphologies of the films also barely changed upon incorporation with Ln^{3+} cations (Figure S5, 6). To determine the chemical states of Ln^{3+} cations in in Tb^{3+}@MIL-100 (In) and Eu^{3+}@MIL-100 (In) films, the Ln^{3+} 4d X-ray photoelectron spectroscopy (XPS) spectra were recorded (Figure S7). The 4d peak positions of Tb^{3+} (148.9 eV) and Eu^{3+} (133.9 eV) in Ln^{3+}@MIL-100 (In) both shift to lower regions in comparison with that of $TbCl_3$ (150.1 eV) and $EuCl_3$ (135.3 eV), suggesting that Ln^{3+} cations are coordinated to the free carboxyl groups of the extra trimesic acid in the cavities.

After postsynthetic functionalization of Ln^{3+} cations, as expected, the MOF films emitted their distinctive colors (Eu^{3+}@MIL-100 (In), red; Tb^{3+}@MIL-100 (In), green), which can be readily observed with the naked eyes as a qualitative indication of sensitization of lanthanide cations (the insets in Figure 2a, b). The luminescence spectra of Ln^{3+}@MIL-100 (In) films are shown in Figure 2. Lanthanides-centered excitation spectra recorded for both Tb^{3+}@MIL-100 (In) (λ_{em} = 544 nm) and Eu^{3+}@MIL-100 (In) (λ_{em} = 615 nm) films display a strong broad band peaking at 297 nm, indicating the presence of energy transfer from the organic linkers to Ln^{3+} cations. Upon excitation at 297 nm, Eu^{3+}@MIL-100 (In) film exhibits sharp emissions centered at 579, 590, 615, 653, 701 nm which are originating from the $^5D_0 \rightarrow {}^7F_J$ (J = 0-4) transitions of Eu^{3+}, while Tb^{3+}@MIL-100 (In) exhibits emissions at 488, 544, 587, and 622 nm which are from the $^5D_4 \rightarrow {}^7F_J$ (J = 6, 5, 4, and 3) transitions of Tb^{3+}. The luminescence lifetimes and quantum yields of Ln^{3+}@MIL-100 (In) films are reasonably high, as demonstrated in Table S1.

To achieve the conceptual barcoding function of Ln^{3+}@MIL-100 (In) films, we designed an encoding strategy based on tuning their emission intensities in multiple bands through a luminescence re-absorbed process (Scheme 1). Specifically, Ln^{3+}@MIL-100 (In) films display multiple emission bands with far less spectra overlap than quantum dots or organic dyes, hence the relative intensity of these emissions can be determined accurately. By loading with a screen layer that containing different amounts of organic dyes, some of these emission bands can be re-absorbed to various degrees, while the others are not absorbed by the filtered dyes and serve as ratiometric references to the re-absorbed emission bands. This permits the establishment of a very large number of ratiometric optical signatures or codes.

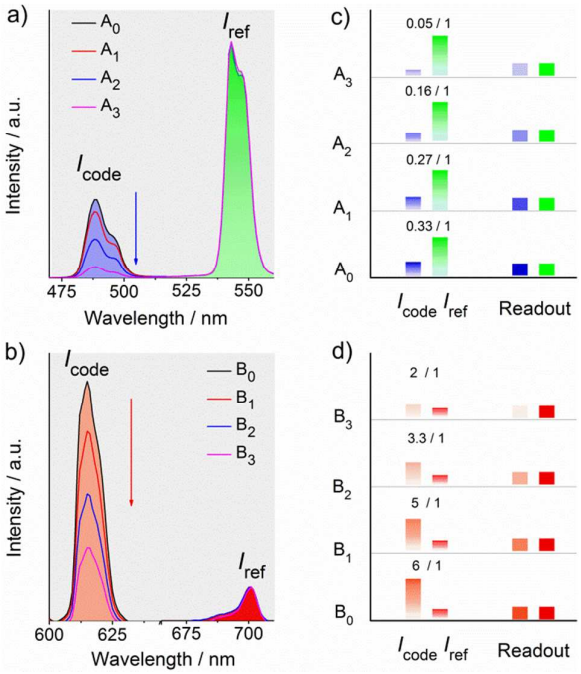

Figure 3. Emission spectra of encoding (a) Tb^{3+}@MIL-100 (In) and (b) Eu^{3+}@MIL-100 (In) films. Both 488 and 615 nm emission (I_{code}) are tuned in four increments by varying the loading concentration of fluorescein isothiocyanate or methylene blue, respectively. In contrast, 544 and 701 nm emissions ($I_{ref.}$) remain constant. Here, the encoding Tb^{3+}@MIL-100 (In) and Eu^{3+}@MIL-100 (In) films are defined as A and B, while their subscripts in A and B are used to differentiate the films with different dye loaded amounts. For instance, A0 and B3 mean Tb^{3+}@MIL-100 (In) film with free fluorescein isothiocyanate loading and Eu^{3+}@MIL-100 (In) film with maximum methylene blue loading, respectively. (c) and (d) are the color-coded schematic of the barcoded readout, which are derived from (a) and (b), respectively.

As shown in Figure 3, two of the emission bands of Ln^{3+}@MIL-100 (In) films (488 and 544 nm emissions for Tb^{3+}@MIL-100 (In), and 616 nm and 701 nm for Eu^{3+}@MIL-100 (In) were employed for the demonstration. Luminescence outside the Ln^{3+} emission bands is basically nonexistent, providing an indication of the low background interference. For the filtered dyes, fluorescein isothiocyanate (FL) and methylene blue (MB) were selected for respective Tb^{3+}@MIL-100 (In) and Eu^{3+}@MIL-100 (In) films for the reasons of high extinction coefficients and overlapping absorption spectra with only one of the two emission bands of Ln^{3+}@MIL-100 (In) films. The adsorption spectra and molecular structure of FL and MB dyes are depicted in Figure S8. The concentrations of the dyes are adjusted in four levels. With an increase in the amount of filtered dyes, the filtered emissions intensities (I_{code}) fall accordingly due to the re-absorbed light processes (Figure 3a and 3b). At high dye concentration, the intensity of I_{code} was reduced up to 15% for Tb^{3+}@MIL-100 (In) and 33% for Eu^{3+}@MIL-100 (In) film compared the isolated Ln^{3+}@MIL-100 (In) films. In contrast, the intensities of unfiltered emissions (I_{ref}) barely change. Thus, we can quantitatively control the resulting ratiometric ratio of the emission intensities (I_{code}/I_{ref}) by manipulating the loading amounts of the filtered dyes. Here, four ratiometric intensity ratios were generated for both Tb^{3+}@MIL-100 (In) and Eu^{3+}@MIL-100 (In) films, which give rise to four optical codes, respectively. To facilitate the interpretation and human qualification, ratiometric optical signals were transferred to color-related codes (Figure 3c and 3d). The emission bands (I_{code}/I_{ref}) are represented by distinctive colors, and their intensities are reflected in the display.

The coding capacity can be increased by using a mixed lanthanide luminescence MOF film. As a first step in this direction, we prepared Eu^{3+}/Tb^{3+}@MIL-100 (In) film by soaking MIL-100 (In) film in the ethanol solution of the mixed chloride salts of Eu^{3+} and Tb^{3+}. The X-ray diffraction pattern (Figure S9) and SEM image (Figure S10) of Eu^{3+}/Tb^{3+}@MIL-100 (In) film indicate that the incorporation of Ln^{3+} cations didn't vary the structure and the morphology of the MOF films. ICP-MS study reveals that the atomic ratios of Tb/In and Eu/In of Eu^{3+}/Tb^{3+}@MIL-100 (In) film are 19.1% and 3.6%, respectively. The emission spectrum of Eu^{3+}/Tb^{3+} film is shown in Figure S11. As expected, it exhibits dual emissions of Eu^{3+} and Tb^{3+} upon excitation at the same wavelength. Three emission bands (488, 544, and 615 nm) of Eu^{3+}/Tb^{3+}@MIL-100 (In) film were chosen as the spectral signals for realizing the barcoding function (Figure 4a). Of them, 488 (I_{code1}) and 615 nm (I_{code2}) emissions were filtered by FL and MB dyes, respectively. On the contrary, 615 nm emission was unfiltered and served as reference (I_{ref}) to the filtered emissions. Similarly, the concentration of FL and MB dyes were both set as four levels, leading to 16 combinations in total. Since the information of the combinations can be carried by their emission intensities in multiple bands, each of the combinations correlates to one two-dimensional ratiometric code (I_{code1}/I_{ref}, I_{code2}/I_{ref}), which is

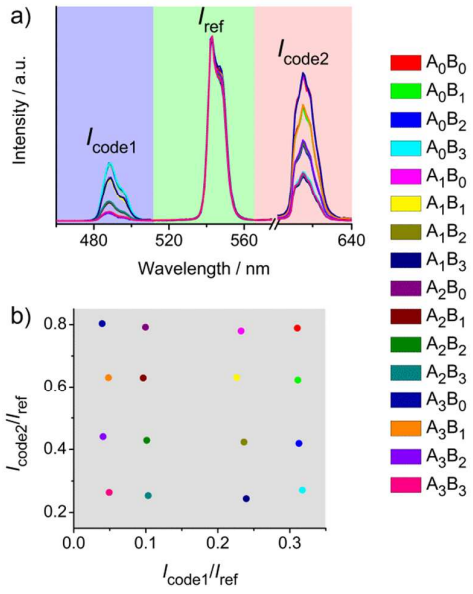

Figure 4. (a) Emission spectra of Eu^{3+}/Tb^{3+}@MIL-100 (In) films with various dyes (FL and MB) loading combinations. The loading concentration of both FL and MB are set as four levels, leading to 4^2 ratiometric codes. (b) Two dimensional matrix of the ratiometric codes derived from a), revealing that the ratiometric codes can be well separated and identified.

calculated by the ratios of two filtered intensities (I_{code1} and I_{code2}) to one reference intensity (I_{ref}). The two -dimensional ratiometric codes were arranged in a matrix (Figure 4b), demonstrating that the optical codes can be well separated and identified. In theory, the number of codes increases exponentially when more emission bands and more intensity levels were used.[40] For instances, four encoded emission bands with 20 increments result in 20^4 codes. An encoding system with 20^4 codes is fascinating, but the difficulties in precise filtered dyes loading also increase, so that a more accurate control must be taken in the synthesis.

Conclusions

In summary, we have described a new straightforward strategy to create barcoded systems based on lanthanides photo-functionalized luminescence MOF films that contain multiple emission bands. By controlling the filtered dyes loading, we can predict and tune the emissions of Ln^{3+}@MIL-100 (In) films in multiple bands and therefore give rise to distinct ratiometric optical codes. This encoding strategy is significantly different from that in the previously reported MOF barcoded systems.[33,34] Spectral encoding relied on lanthanides luminescence offers a range of advantages over organic fluorophores and quantum dots, such as low spectra and background interference, and self-referencing. With expansion of the available coded emission bands and their intensity levels, the coding capability increases exponentially. Our current work is focused on tailoring the encoded films into micrometer scale such that they can potentially be used in the practical applications of anti-counterfeiting, massively parallelized bioassays, and forensic labelling.

Acknowledgements

This work was supported by the National Natural Science Foundation of China (91122003), Developing Science Funds of Tongji University and the Science & Technology Commission of Shanghai Municipality (14DZ2261100).

Notes and references

1 D. H. Park, Y. K. Hong, E. H. Cho, M. S. Kim, D. C. Kim, J. Bang, J. Kim and J. Joo, *Acs Nano*, 2010, **4**, 5155.
2 X. F. Zhang, Y. Xiao, L. He and Y. H. Zhang, *J. Org. Chem.*, 2014, **79**, 6315.
3 P. O. Krutzik and G. P. Nolan, *Nat. Methods*, 2006, **3**, 361.
4 L. Wang and W. H. Tan, *Nano letters*, 2006, **6**, 84.
5 M. Y. Han, X. H. Gao, J. Z. Su and S. Nie, *Nat. Biotechnol.*, 2001, **19**, 631.
6 C. Chen, P. F. Zhang, G. H. Gao, D. Y. Gao, Y. Yang, H. Liu, Y. H. Wang, P. Gong and L. T. Cai, *Adv. Mater.*, 2014, **26**, 6313.
7 Y. J. Zhao, H. C. Shum, H. S. Chen, L. L. A. Adams, Z. Z. Gu and D. A. Weitz, *J. Am. Chem. Soc.*, 2011, **133**, 8790.
8 Y. J. Zhao, Z. Y. Xie, H. C. Gu, L. Jin, X. W. Zhao, B. P. Wang and Z. Z. Gu, *NPG Asia Mater.*, 2012, **4**, e25.
9 S. Rauf, A. Glidle and J. M. Cooper, *Adv. Mater.*, 2009, **21**, 4020.
10 J. Ya X. G. Peng, *Accounts Chem. Res.*, 2010, **43**, 1387.
11 A. M. Smith, A. M. Mohs and S. Nie, *Nat. Nanotechnol.*, 2009, **4**, 56.
12 J. Yang, S. R. Dave and X. H. Gao, *J. Am. Chem. Soc.*, 2008, **130**, 5286.
13 J. C. G. Bunzli and C. Piguet, *Chem. Soc. Rev.*, 2005, **34**, 1048.
14 J. Lee, P. W. Bisso, R. L. Srinivas, J. J. Kim, A. J. Swiston and P. S. Doyle, *Nat. Mater.*, 2014, **13**, 524.
15 H. H. Gorris, R. Ali, S. M. Saleh and O. S. Wolfbeis, *Adv. Mater.*, 2011, **23**, 1652.
16 F. Zhang, Q. H. Shi, Y. C. Zhang, Y. F. Shi, K. L. Ding, D. Y. Zhao and G. D. Stucky, *Adv. Mater.*, 2011, **23**, 3775.
17 Q. B. Zhang, X. Wang and Y. M. Zhu, *J. Mater. Chem.*, 2011, **21**, 12132.
18 Y. J. Cui, Y. F. Yue, G. D. Qian and B. L. Chen, *Chem. Rev.*, 2012, **112**, 1126.
19 X. J. Zhang, W. J. Wang, Z. J. Hu, G. N. Wang and K. S. Uvdal, *Coord. Chem. Rev.*, 2015, **284**, 206.
20 Z. C. Hu, B. J. Deibert and J. Li, *Chem. Soc. Rev.,* 2014, **43**, 5815.
21 Y. J. Cui, B. L. Chen and G. D. Qian, *Coord. Chem. Rev.*, 2014, **273**, 76.
22 J. Rocha, L. D. Carlos, F. A. A. Paz and D. Ananias, *Chem. Soc. Rev.,* 2011, **40**, 926.
23 B. L. Chen, L. B. Wang, Y. Q. Xiao, F. R. Fronczek, M. Xue, Y. J. Cui and G. D. Qian, *Angew. Chem., Int. Edit.*, 2009, **48**, 500.
24 G. Lu and J. T. Hupp, *J. Am. Chem. Soc.*, 2010, **132**, 7832.
25 Y. Zhou, B. Yan and F. Lei, *Chem. Commun.*, 2014, **50**, 15235.
26 Y. Zhou, H. H. Chen and B. Yan, *J. Mater. Chem. A*, 2014, **2**, 13691.
27 Y. Lu and B. Yan, *Chem. Commun.*, 2014, **50**, 13323.
28 C. Y. Sun, X. L. Wang, X. Zhang, C. Qin, P. Li, Z. M. Su, D. X. Zhu, G. G. Shan, K. Z. Shao, H. Wu and J. Li, *Nat. Commun.*, 2013, **4**, 2717.
29 Y. Liu, M. Pan, Q. Y. Yang, L. Fu, K. Li, S. C. Wei and C. Y. Su, *Chem. Mater.*, 2012, **24**, 1954.
30 J. He, M. Zeller, A. D. Hunter and Z. T. Xu, *J. Am. Chem. Soc.*, 2012, **134**, 1553.
31 Y. Lu and B. Yan, *Chem. Commun.*, 2014, **50**, 15443.
32 Y. Zhou and B. Yan, *Nanoscale*, 2015, **7**, 4063.
33 K. A. White, D. A. Chengelis, K. A. Gogick, J. Stehman, N. L. Rosi and S. Petoud, *J. Am. Chem. Soc.*, 2009, **131**, 18069.
34 Y. Lu and B. Yan, *J. Mater. Chem. C*, 2014, 2, 7411.
35 Z. S. Dou, J. C. Yu, Y. J. Cui, Y. Yang, Z. Y. Wang, D. R. Yang and G. D. Qian, *J. Am. Chem .Soc.,* 2014, **136**, 5527.
36 J. L. Schlenker, F. G. Dwyer, E. E. Jenkins, W. J. Rohrbaugh, G. T. Kokotailo, *Nature* 1981, **294**, 340.
37 C. Volkringer, D. Popov, T. Loiseau, G. Ferey, M. Burghammer, C. Riekel, M. Haouas and F. Taulclle, *Chem.Mater.*, 2009, **21**, 5695.
38 C. Volkringer, H. Leclerc, J. C. Lavalley, T. Loiseau, G. Ferey, M. Daturi and A. Vimont, *J. Phys. Chem. C*, 2012, **116**, 5710.
39 Z. S. Dou, J. C. Yu, H. Xu, Y. J. Cui, Y. Yang and G. D. Qian, *Microporous and Mesoporous Mater.*, 2013, **179**, 198.
40 R. Wilson, A. R. Cossins and D. G. Spiller, *Angew. Chem., Int. Edit.*, 2006, **45**, 6104.

Table of Contents

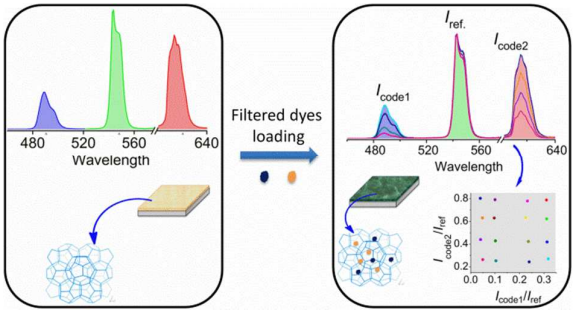

Luminescence MOF films based ratiometric multiplexed barcodes were demonstrated in this work. The encoding strategy is based on tuning the emission intensity in multiple emission bands of lanthanides by controlling filtered dyes loading, which represents a straightforward approach for lanthanides luminescence MOFs to generate ratiometric barcodes in a robust and reproducible way.